The EMBO Journal (2012) 31, 187–200 | © 2012 European Molecular Biology Organization | All Rights Reserved 0261-4189/12
www.embojournal.org

THE EMBO JOURNAL

Quantitative modelling of amyloidogenic processing and its influence by SORLA in Alzheimer's disease

Vanessa Schmidt[1], Katharina Baum[1,6], Angelyn Lao[2,6], Katja Rateitschak[2], Yvonne Schmitz[2], Anke Teichmann[3], Burkhard Wiesner[3], Claus Munck Petersen[4], Anders Nykjaer[4], Jana Wolf[1], Olaf Wolkenhauer[2,5,*] and Thomas E Willnow[1,*]

[1]Max-Delbrück-Center for Molecular Medicine, Berlin, Germany, [2]Department of Systems Biology and Bioinformatics, Institute of Computer Science, University of Rostock, Rostock, Germany, [3]Leibniz-Institut für Molekulare Pharmakologie, Berlin, Germany, [4]MIND Center, Department of Biomedicine, University of Aarhus, Aarhus C, Denmark and [5]Stellenbosch Institute for Advanced Study (STIAS), Stellenbosch, South Africa

The extent of proteolytic processing of the amyloid precursor protein (APP) into neurotoxic amyloid-β (Aβ) peptides is central to the pathology of Alzheimer's disease (AD). Accordingly, modifiers that increase Aβ production rates are risk factors in the sporadic form of AD. In a novel systems biology approach, we combined quantitative biochemical studies with mathematical modelling to establish a kinetic model of amyloidogenic processing, and to evaluate the influence by SORLA/SORL1, an inhibitor of APP processing and important genetic risk factor. Contrary to previous hypotheses, our studies demonstrate that secretases represent allosteric enzymes that require cooperativity by APP oligomerization for efficient processing. Cooperativity enables swift adaptive changes in secretase activity with even small alterations in APP concentration. We also show that SORLA prevents APP oligomerization both in cultured cells and in the brain *in vivo*, eliminating the preferred form of the substrate and causing secretases to switch to a less efficient non-allosteric mode of action. These data represent the first mathematical description of the contribution of genetic risk factors to AD substantiating the relevance of subtle changes in SORLA levels for amyloidogenic processing as proposed for patients carrying *SORL1* risk alleles.

The EMBO Journal (2012) **31,** 187–200. doi:10.1038/emboj.2011.352; Published online 11 October 2011
Subject Categories: membranes & transport; neuroscience; molecular biology of disease

Keywords: amyloidogenic processing; LR11; secretases; SORL1; VPS10P domain receptors

*Corresponding authors. O Wolkenhauer, Department of Systems Biology and Bioinformatics, Institute of Computer Science, University of Rostock, Ulmenstrasse 69, 18057 Rostock, Germany. Tel.: + 49 381 498 7571; Fax: + 49 381 498 7572; E-mail: olaf.wolkenhauer@uni-rostock.de
or TE Willnow, Max-Delbrück-Center for Molecular Medicine, Robert-Roessle-Str. 10, D-13125 Berlin, Germany. Tel.: + 49 30 9406 2569; Fax: + 49 30 9406 3382; E-mail: willnow@mdc-berlin.de
[6]These authors contributed equally to this work

Received: 3 March 2011; accepted: 5 September 2011; published online: 11 October 2011

Introduction

According to the amyloid hypothesis, the extent of proteolytic processing of the amyloid precursor protein (APP) into amyloid-β (Aβ) peptides is central to the pathology of Alzheimer's disease (AD) (Haass and Selkoe, 2007). Support for this concept not only comes from familial cases of AD in which mutations in the genes encoding APP and presenilins profoundly alter APP processing fates (Hardy, 2009). This hypothesis is also supported by data from sporadic forms of the disease where more subtle changes in the activity of modifiers are believed to promote production of neurotoxic Aβ species. A number of modifier genes have been shown to affect APP processing fates including LRP1 (Pietrzik *et al*, 2002), Nogo-66 receptor (Park and Strittmatter, 2007), or Bri2 (Matsuda *et al*, 2005), just to name a few. However, their relevance for AD has mostly been investigated in transgenic cell lines and in knockout mouse models. While these studies were important to identify basic concepts in APP processing, experimental systems with massive overexpression or complete lack of modifier activity fall short of modelling the *in vivo* situation in patients where modest alterations in activity may affect neuropathology over the course of a life time.

Sorting protein-related receptor with A-type repeats (SORLA; also known as SORL1 or LR11) is a neuronal receptor for APP that controls intracellular transport and processing of the precursor protein (Andersen *et al*, 2005; Offe *et al*, 2006; Schmidt *et al*, 2007). In cultured cells, SORLA impairs the initial cleavage of APP by α- and β-secretases, blocking amyloidogenic and non-amyloidogenic processing pathways alike (Schmidt *et al*, 2007). Since expression of SORLA is reduced in the brain of some patients with sporadic AD (Dodson *et al*, 2006) and because *SORL1* gene variants are associated with occurrence of the disease (Rogaeva *et al*, 2007), the receptor is considered a major risk gene in late-onset AD (Bertram *et al*, The AlzGene Database; http://www.alzgene.org).

To test the relevance of even subtle alterations in SORLA levels for amyloidogenic processing, we developed a unique cell system, where we can vary the molar ratio of APP and SORLA over a continuous range of concentrations—a model that more truly reflects the situation in AD patients than knockout or overexpression experiments. In a systems biology approach, we combined quantitative biochemical studies with mathematical modelling to establish the first kinetic model of APP processing and its influence by SORLA. Our data demonstrate that α- and β-secretases are allosteric

enzymes that depend on the formation of APP oligomers for efficient processing. Cooperativity in APP binding enables swift adaptive changes in enzyme activity with even small alterations in substrate concentration. We also demonstrate that SORLA does not affect the enzymatic activity of secretases *per se*. Rather, it acts as inhibitor that prevents APP oligomerization, thereby eliminating the preferred form of the secretase substrate and reducing amyloidogenic processing.

Results

Application of Tet-off system to modulate SORLA and APP expression levels

We have applied the tetracycline-controlled transactivator (tTA) system to develop a cellular model with tightly controlled expression of APP and SORLA over a wide range of molar concentrations. In the Tet-off version of this system (Gossen and Bujard, 1992), constitutive expression of transgenes (such as APP and SORLA) is driven from a regulatory site composed of the modified tetracycline-response element (TRE_{MOD}) and a minimal CMV promoter (Figure 1A). Transcription requires binding of tTA to TRE_{MOD}. The application of doxycycline releases tTA from the promoter and shuts off gene transcription in a dose-dependent manner (Figure 1A). The Tet-off system worked faithfully to vary the molar concentrations of APP and SORLA in Chinese hamster ovary (CHO) cells transfected with the respective expression constructs. Thus, application of doxycycline resulted in stable reduction of APP and SORLA protein levels in cells after 24 h (Figure 1B). As shown by immunofluorescence microscopy (Supplementary Figure S1), the recombinant proteins co-localized to the perinuclear (Golgi) region, the main cellular compartment where both proteins interact in cultured cells and in tissues *in vivo* (Offe *et al*, 2006; Rogaeva *et al*, 2007; Schmidt *et al*, 2007). Doxycycline-induced repression of one of the proteins (here APP) did not affect expression and subcellular localization of the constitutively expressed partner (here SORLA; Supplementary Figure S1B).

Next, expression constructs for doxycycline-regulatable expression of APP and SORLA were stably introduced into parental CHO cells or into CHO cells constitutively expressing human SORLA (CHO-S) or APP_{695} (CHO-A) (Schmidt *et al*, 2007). All in all, three types of cell lines were generated: (i) CHO pTet-APP to control APP expression in the absence of SORLA, (ii) CHO-S pTet-APP to regulate APP levels at constant concentrations of SORLA, and (iii) CHO-A pTet-SORLA to regulate SORLA levels at a fixed concentration of APP (Figure 2A). Applying a range of doxycycline concentrations from 0.025 to 10 ng/ml for 48 h enabled us to modify the cellular concentrations of APP (from pTet-APP) and of SORLA (from pTet-SORLA) in a dose-dependent manner as shown by western blot analysis (Figure 2A) and ELISA (Figure 2B). Down-regulation worked best for pTet-APP with

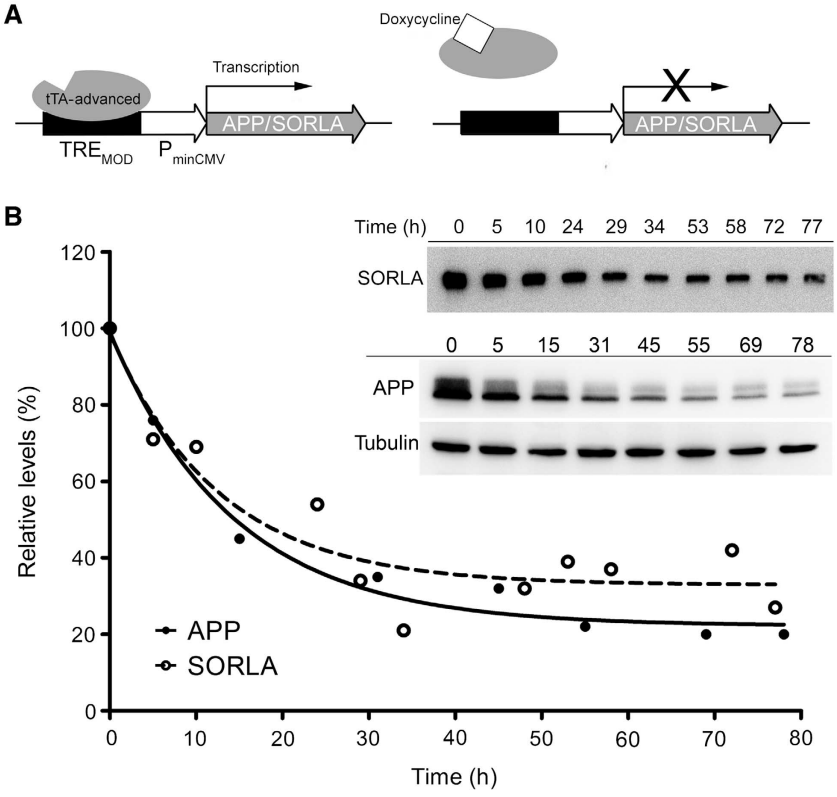

Figure 1 Tet-off system to modulate cellular expression of APP and SORLA. (**A**) Strategy for doxycycline-dependent repression of APP and SORLA expression using the Tet-off system. tTA, tetracycline-controlled transactivator. (**B**) CHO cells were stably transfected with Tet-off constructs for expression of SORLA and APP. Following treatment with 1 ng/ml doxycycline for the indicated periods of time, expression levels of both proteins were determined by western blot analysis as exemplified in the inset. Intensities of the immunoreactive bands corresponding to SORLA and APP were quantified by densitometric scanning in replicate blots ($n = 3$), and expressed as relative levels compared with untreated cells (set at 100%). Error bars are smaller than the actual data symbols shown.

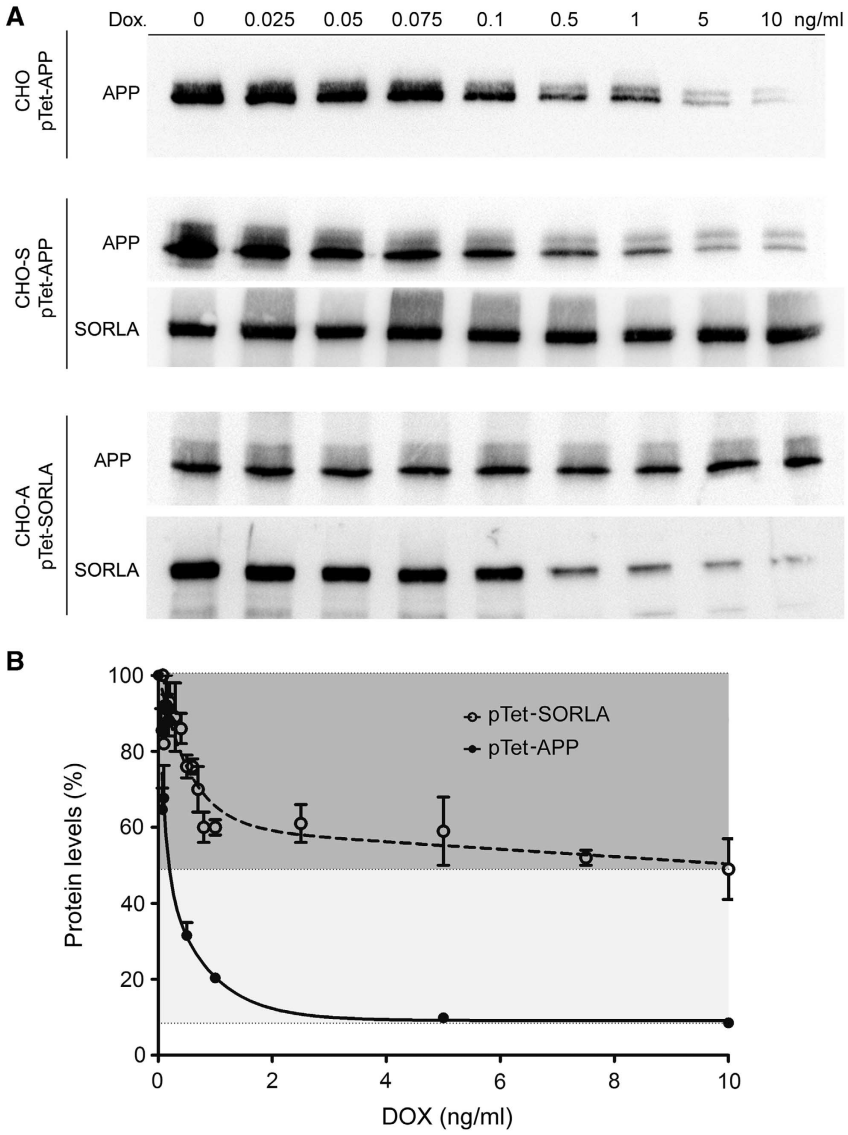

Figure 2 CHO cell models with regulatable expression of SORLA and APP. (**A**) Parental CHO cells or CHO cells constitutively expressing human SORLA (CHO-S) or APP_{695} (CHO-A) were stably transfected with Tet-off constructs for APP (pTet-APP) or SORLA (pTet-SORLA). Protein expression was detected in lysates from cells treated with the indicated concentrations of doxycycline for 48 h. (**B**) Quantification by ELISA of APP and SORLA expressed from the Tet-off constructs following doxycycline treatment (four independent repeats). Protein levels are indicated as percent of levels seen in the untreated conditions (set at 100%).

a 90% reduction of expression at 10 ng/ml of doxycycline. pTet-SORLA levels were reduced by ~50% at maximal doxycycline concentration (Figure 2B). The residual levels of APP and SORLA seen in transfectants at 10 ng/ml of doxycycline (Figure 2A) represented leaky expression from the Tet-off constructs as no signals corresponding to the endogenous proteins were seen in parental CHO cells (Supplementary Figure S2). Accordingly, all analyses in this study relate to the cellular interaction of human APP and human SORLA.

SORLA alters the mode of secretase action from allosteric to non-allosteric

Initially, we applied cell lines CHO pTet-APP and CHO-S pTet-APP to describe the kinetics of α- and β-secretase activities in our cell model in the presence or absence of SORLA. Replicate cell layers were subjected to a range of doxycycline concentrations and the concentration of the substrate APP in the corresponding cell lysates was correlated with the rate of production of soluble (s) APPα and sAPPβ, the products of α- and β-secretase activities, respectively. Surprisingly, in cells without SORLA (CHO pTet-APP), the Michaelis–Menten equation failed to correctly describe the enzyme kinetics as shown by the deviation of data points from the calculated hyperbolic curve (closed symbols, Figure 3A and B), and by the high absolute error (Table IA). Instead, a more accurate fit of the data points (closed symbols, Figure 3C and D) and a reduction in absolute error (Table IA) was obtained when we used a Hill equation. Hill kinetics describe cooperativity in (allosteric) enzyme activity and are characterized by a sigmoidal relationship of substrate concentration with enzyme reaction rate. The Hill coefficient, describing the degree of cooperativity, was 2 for both α- and β-secretases, suggesting dimerization of enzymes or substrate (or both) as determinant of enzyme kinetics (Table IA).

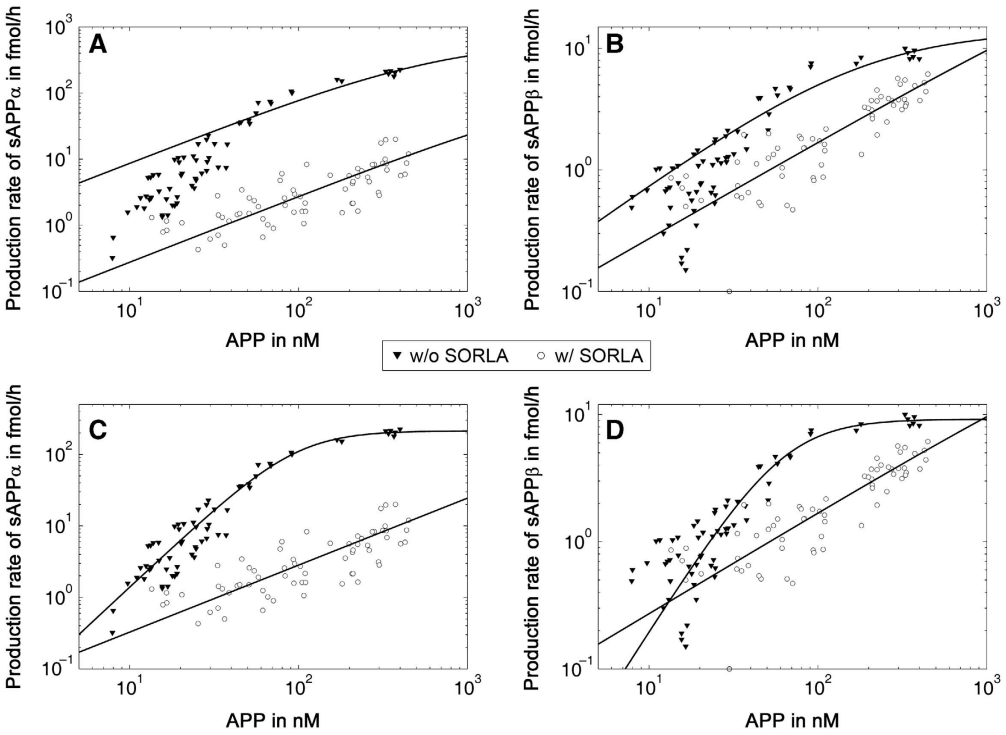

Figure 3 Enzyme kinetics of soluble APP production in the presence or absence of SORLA. CHO pTet-APP (w/o SORLA) and CHO-S pTet-APP (w/ SORLA) cells were treated with a concentration range of 0.025–10 ng/ml of doxycycline for 48 h. Subsequently, concentrations of APP in cell lysates and total amount of soluble (s) APPα (**A**, **C**) and sAPPβ (**B**, **D**) secreted into the medium within 24 h were determined by ELISA. Enzyme kinetics of APP turnover into sAPP products was calculated using Michaelis–Menten (**A**, **B**) or Hill equations (**C**, **D**). Log scale presentation was chosen to better illustrate the deviation of data points from the calculated curve for CHO pTet-APP (closed symbols) for Michaelis–Menten kinetics (**A**, **B**) compared with the Hill equation (**C**, **D**).

Table I Comparison of Hill and Michaelis–Menten kinetics for α- and β-secretases in cells without (A) and with (B) SORLA

	Michaelis–Menten		Hill	
	α-Secretase	β-Secretase	α-Secretase	β-Secretase
(A) w/o SORLA				
Absolute error	13 940.0	45.9	3306.8	19.0
Hill coefficient	—	—	2.21	2.09
(B) w/ SORLA				
Absolute error	573.7	28.8	573.1	28.4
Hill coefficient	—	—	0.94	0.79

The presence of SORLA (in CHO-S pTet-APP) reduced the total amount of soluble APP products generated from APP drastically as compared with CHO pTet-APP (Figure 4). At half-maximal velocity ($V_{0.5}$) of α-secretase, the amount of sAPPα produced from 106.9 nM APP was reduced from 97.2 to 2.7 fmol/h in the presence of 120 nM SORLA (97% reduction) (Figure 4A). Similarly, the amount of sAPPβ produced from 62.6 nM APP ($V_{0.5}$ of β-secretase) was reduced from 4.6 to 1.1 fmol/h in the presence of 120 nM SORLA (75% reduction) (Figure 4B).

Surprisingly, the presence of SORLA also profoundly changed the mode of secretase action from allosteric to non-allosteric. Thus, the requirement for cooperativity was lost when cells expressed the receptor as shown by a similar curve fit and identical absolute errors when applying Michaelis–Menten (open symbols, Figure 3A and B; Table IB) or Hill (open symbols, Figure 3C and D; Table IB) equations. Lack of cooperativity in APP processing with SORLA was also confirmed by Hill coefficients of 0.97 and 0.79 for α- and β-secretases, respectively (Table IB).

The necessity for cooperativity and loss thereof in the presence of SORLA was also seen when studying the kinetics of Aβ production in CHO pTet-APP versus CHO-S pTet-APP cells. As has been observed for α- and β-secretases above (Figure 3), Hill but not Michaelis–Menten equations correctly described the γ-secretase kinetics in the absence of the SORLA (closed symbols, Figure 5A versus B). In contrast in the presence of SORLA, a similar curve fit was obtained when applying Michaelis–Menten (open symbols, Figure 5A) or Hill (open symbols, Figure 5B) equations. Overall, the extent of $Aβ_{40}$ production at 35.4 nM APP ($V_{0.5}$) was reduced from 18.7 fmol/h in CHO pTet-APP to 0.77 fmol/h in the presence of 120 nM SORLA in CHO-S pTet-APP (96% reduction) (Figure 5C).

Inverse correlation between SORLA activity and APP processing rates

Previous studies had demonstrated a 25% reduction in SORLA levels in the brain of some patients suffering from sporadic AD (Scherzer *et al*, 2004). Whether such modest alterations in receptor level may have any functional consequences for amyloidogenic processing remained controversial. To unambiguously test the relevance of even small variations in SORLA activity for APP processing, we applied another cell line CHO-A pTet-SORLA. In this cell model, the ratio of substrate APP and secretases is kept constant but the

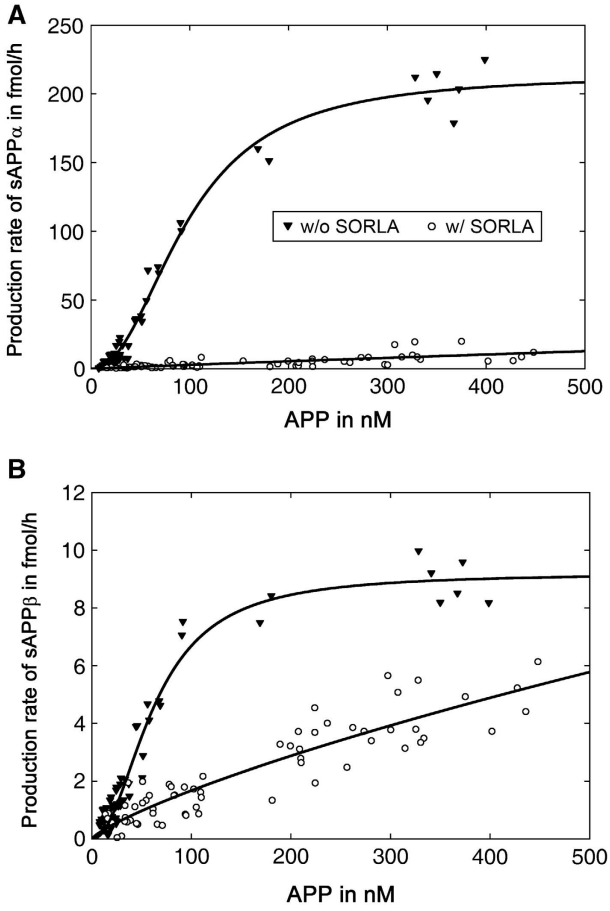

Figure 4 Inhibitory effect of SORLA on soluble APP production. CHO pTet-APP (w/o SORLA) and CHO-S pTet-APP (w/ SORLA) cells were treated with a concentration range of 0.025–10 ng/ml doxycycline for 48 h. Then, concentrations of APP in the cell lysates and total amount of sAPPα (**A**) and sAPPβ (**B**) secreted into the medium within 24 h were determined by ELISA. Enzyme kinetics were calculated using a Hill equation. These data are identical to the data points shown in Figure 3 but linear presentation was chosen here to better illustrate the dramatic decrease in APP processing in cells expressing SORLA (open symbols) compared with parental CHO cells (closed symbols).

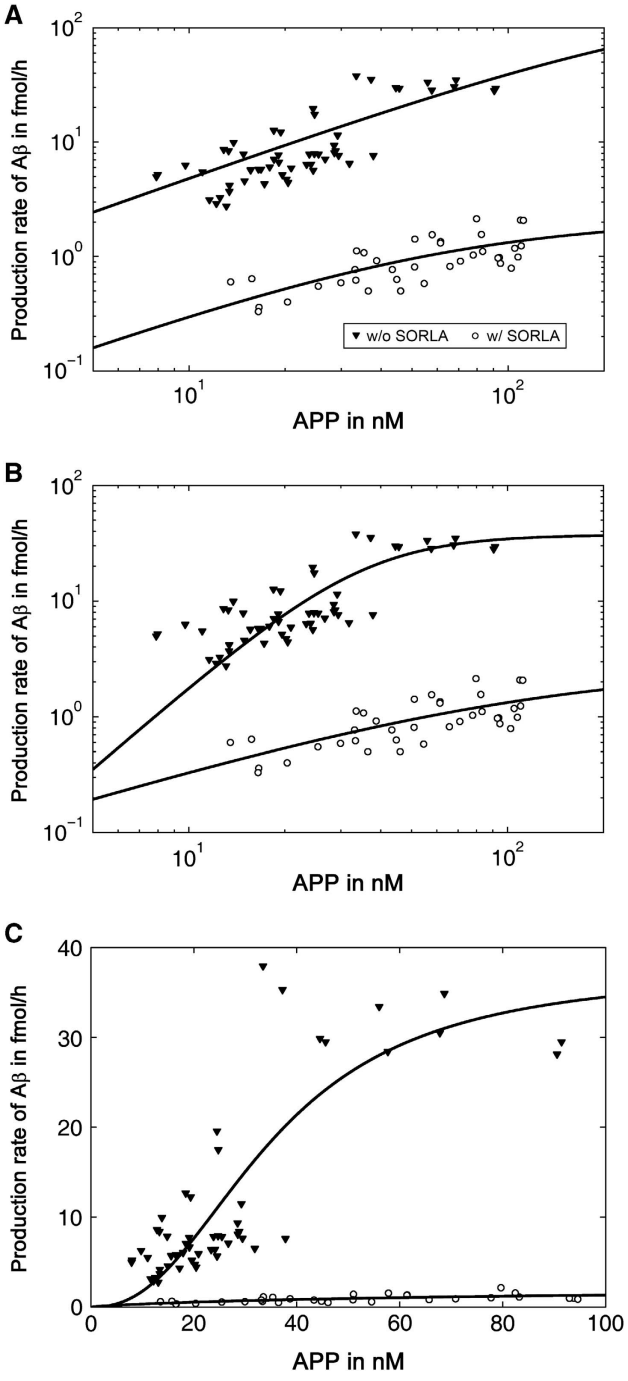

Figure 5 Kinetics of $A\beta_{40}$ peptide production in the presence or absence of SORLA. (**A**, **B**) CHO pTet-APP (w/o SORLA) and CHO-S pTet-APP (w/ SORLA) cells were treated with a concentration range of 0.025–10 ng/ml doxycycline for 48 h. Subsequently, concentrations of APP in the cell lysates and the total amount of $A\beta_{40}$ secreted into the medium within 24 h were determined by ELISA. Enzyme kinetics of substrate APP turnover into $A\beta_{40}$ was calculated using Michaelis–Menten (**A**) or Hill equations (**B**). Log scale presentation was chosen to better illustrate the deviation of data points from the calculated curve for CHO pTet-APP (closed symbols) for Michaelis–Menten kinetics (**A**) compared with the Hill equation (**B**). (**C**) Enzyme kinetics as in (**B**) were calculated using a Hill equation. However, linear presentation of data points was chosen to better illustrate the dramatic decrease in $A\beta_{40}$ production in cells expressing SORLA (open symbols) compared with parental CHO cells (closed symbols).

molar concentration of the inhibitor SORLA is altered. Although the molar ratio of doxycycline-regulatable SORLA to constitutively expressed APP could only be varied 2.5-fold (50% reduction in SORLA), a clear inverse correlation of SORLA levels with rates of APP processing into sAPPα, sAPPβ, and $A\beta_{40}$ was seen along the entire concentration range (Figure 6).

To test whether a similar inverse relationship between SORLA activity and APP processing is also seen for the endogenous proteins in neurons, we established siRNA knockdown of receptor expression in the human neuroblastoma cell line SH-SY5Y that expresses endogenous levels of SORLA and APP (Figure 7A, inset). As shown for CHO cells above (Figure 6), a clear inverse correlation of SORLA levels with production rates for sAPPα, sAPPβ, and $A\beta_{40}$ was also observed in SH-SY5Y (Figure 7). These data substantiated the relevance of subtle changes in SORLA activity for the extent of APP processing as proposed for patients carrying *SORL1* risk alleles (Scherzer *et al*, 2004; Rogaeva *et al*, 2007).

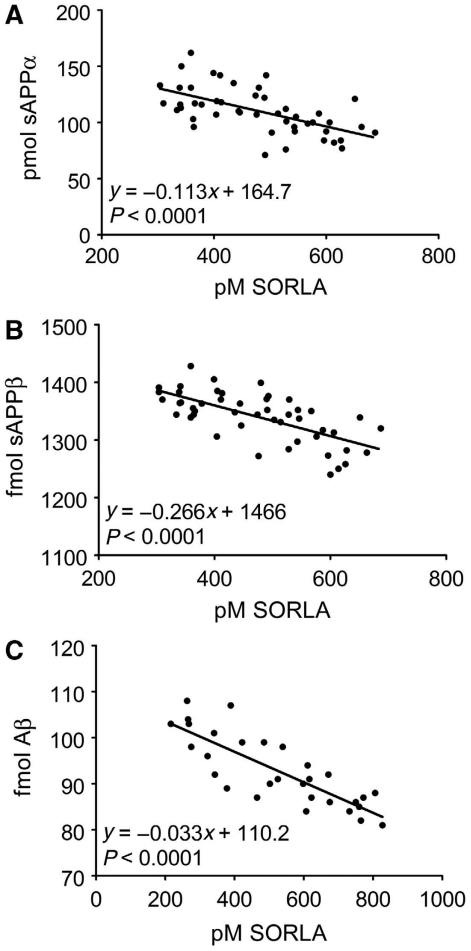

Figure 6 SORLA is a dose-dependent inhibitor of APP processing in CHO cells. CHO-A pTet-SORLA cells were treated with a concentration range of 0.025–60 ng/ml doxycycline for 48 h. Thereafter, the concentrations of SORLA in cell lysate and of the total amounts of soluble (s) APPα, sAPPβ, and of $Aβ_{40}$ secreted into the medium within 24 h were determined by ELISA. Linear regression analysis demonstrates a statistically significant linear decrease in the production of sAPPα (**A**), sAPPβ (**B**), and $Aβ_{40}$ (**C**), with increasing SORLA concentrations in the cells.

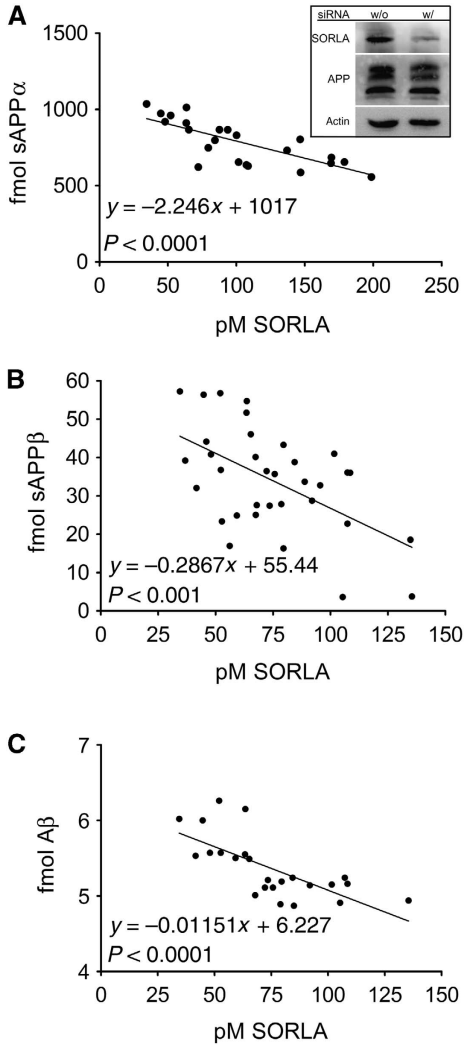

Figure 7 Endogenous SORLA is a dose-dependent inhibitor of APP processing in neuronal cells. (**A**–**C**) Knockdown by siRNA approach was used to modulate the levels of SORLA in the human neuroblastoma cell line SH-SY5Y that expresses SORLA and APP endogenously. Concentration of SORLA in replicate cell lysates and of the respective levels of soluble (s) APPα, sAPPβ, and of $Aβ_{40}$ secreted into the medium within 24 h were determined by ELISA. Linear regression analysis demonstrates a statistically significant linear decrease in the production of sAPPα (**A**), sAPPβ (**B**), and $Aβ_{40}$ (**C**), with increasing SORLA concentrations in the cells. (Inset in **A**) The amount of endogenous APP and SORLA in lysates of cells treated with (w/) or without (w/o) siRNA is shown by western blot analysis. Multiple immunoreactive bands for APP correspond to the immature and mature precursor variants. Detection of actin was used as a loading control.

SORLA does not directly impact enzymatic activity of secretases

So far, our data provided evidence for cooperativity in cleavage of APP by α-, β-, and γ-secretases, and the ability of SORLA to interfere with processing by preventing cooperativity in a dose-dependent manner. Conceptually, these data may be explained by direct binding of SORLA to APP or to the secretases preventing oligomerization of substrate and/or enzymes. The ability of SORLA to bind to APP had been established *in vitro* and in cells by us and others before (Andersen *et al*, 2005, 2006; Offe *et al*, 2006; Spoelgen *et al*, 2006). Here, we explored whether the receptor may also directly interact with secretases to block their enzymatic activity. To do so, we subjected cell lysates of parental CHO cells or CHO-S cells (containing 120 nM SORLA) to cell-free secretase assays. The total amount of tumour necrosis factor converting enzyme (TACE), of ADAM10, and of β-site of APP cleaving enzyme (BACE1) expressed in both cell lines was identical (Figure 8, insets). Also, both cell lines showed similar activities for α-secretase (Figure 8A) and β-secretase (Figure 8B) when applying artificial protease substrates (as described in the Supplementary data).

We also tested the activity of γ-secretase by transiently transfecting expression constructs encoding the carboxyl terminal fragments (CTFs) C83 and C99 into CHO and CHO-S cell lines (Figure 9). C83 and C99 are γ-secretase substrates derived from cleavage of the APP holoprotein by α- and β-secretase, respectively. Forty-eight hours after transfection, cell extracts from CHO and CHO-S cells were generated and incubated for 2 h at 37 °C to determine turnover of CTFs into the APP intracellular domain (AICD) (Figure 9A). Densitometric scanning of replicate western blot experiments

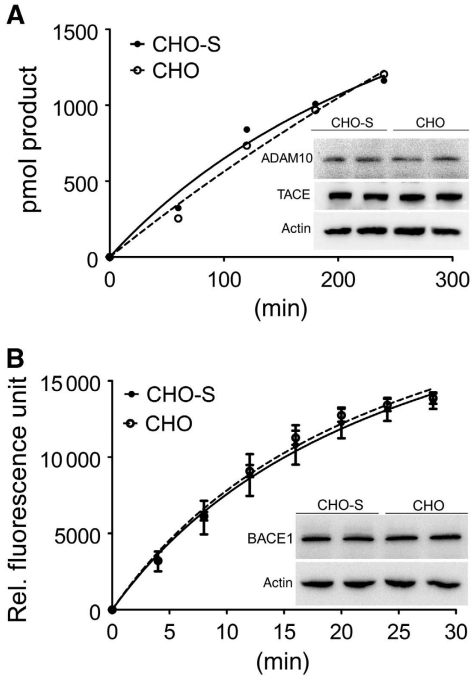

Figure 8 Influence of SORLA on α- and β-secretase activities. Extracts from parental CHO cells and from cells constitutively expressing 120 nM SORLA (CHO-S) were subjected to cell-free α- (**A**) and β-secretase (**B**) activity measurement using commercially available assays (four independent repeats). (Insets) The amount of proposed α-secretases TACE and ADAM10, and of β-secretase BACE1 in both cell lines was evaluated in replicate samples by western blotting. Detection of actin was used as a loading control.

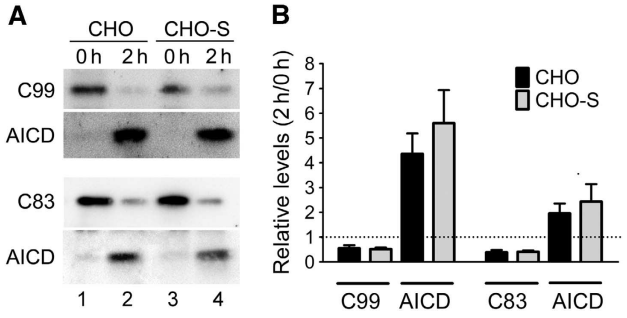

Figure 9 Influence of SORLA on γ-secretase activity. (**A**) Parental CHO cells (lanes 1 and 2) and CHO cells expressing 120 nM SORLA (CHO-S; lanes 3 and 4) were transiently transfected with expression constructs for C99 or C83 for 48 h. Thereafter, cell lysates were either kept on ice (0 h time point) or incubated for 2 h at 37 °C, and the amount of substrates C99/C83 and of the product AICD in the extracts were determined by western blot. (**B**) The intensity of immunoreactive bands representing the indicated proteins were quantified by densitometric scanning and expressed as relative ratio at 2 versus 0 h of incubation. The stippled line indicates a ratio of 1 (2 h/0 h), assuming the absence of γ-secretase activity (three independent repeats).

demonstrated identical γ-secretase activities in cells with or without SORLA (Figure 9B).

SORLA disrupts oligomerization of APP

Taken together, our data demonstrated that SORLA acts as inhibitor of amyloidogenic processing mainly by functionally interacting with APP. Given the requirement for cooperativity in APP processing, we speculated that efficient proteolytic breakdown of APP requires oligomerization of the precursor protein and that binding of SORLA to APP may prevent this from happening. Our hypothesis was confirmed when we studied APP oligomerization in CHO cells in the presence or absence of SORLA. Thus, we transiently expressed a fusion protein of APP with enhanced green fluorescence protein (EGFP) in CHO and CHO-S cells and subjected cell extracts of the transfectants to native polyacrylamide gel electrophoresis (PAGE). Detection of APP–EGFP by fluorescence scanning of the gels or by immunodetection using anti-GFP antiserum demonstrated the presence of monomeric and oligomeric variants of APP–EGFP in parental CHO cells. However, no APP–EGFP oligomers were seen in CHO-S (Figure 10A). The ability of SORLA to block APP homomer formation was substantiated in neuronal cells using fluorescence correlation spectroscopy (FCS). FCS is an analytic tool that enables both qualitatively and quantitatively, examining the molecular dynamics of protein–protein interactions by determining the fluctuation in fluorescence intensities of moving fluorescent molecules (Elson, 2001). When APP–GFP and APP–RFP were co-expressed in parental SH-SY5Y cells, the normalized cross-correlation curve indicated a substantial extent of heterodimer formation between the two APP variants (Figure 10B). In contrast, in SH-SY5Y cells expressing a SORLA transgene cross-correlation represented random noise, demonstrating independent fluctuation of the two protein species (Figure 10C). Quantification of the extent of cross-correlation showed that 30% of all APP molecules represented APP–RFP/APP–GFP dimers in cells without SORLA. Cells expressing the receptor exhibited significantly reduced dimer formation ($P = 0.0067$; inset in Figure 10C).

Finally, to also explore the relevance of SORLA activity for APP dimerization *in vivo*, we applied Blue Native PAGE to brain tissues from wild-type and SORLA-deficient mice (Figure 10D). Remarkably, two immunoreactive bands likely corresponding to monomeric and oligomeric forms of APP were seen in wild-type brain extracts. In contrast, mainly the higher-molecular weight complex of APP was detected in tissue from *Sorla*$^{-/-}$ animals, suggesting increased APP complex formation in the absence of SORLA.

Mathematical modelling of APP processing in the presence or absence of SORLA

Based on the published findings and on our experimental evidence discussed above, we established a biochemical reaction network that describes the kinetics of APP processing and the effect of SORLA on these processes (Figure 11A). The assumptions of the biochemical reaction network were as follows: (i) APP as well as α- and β-secretases exist in an equilibrium of monomeric and homodimeric forms; (ii) SORLA can reversibly form a complex with monomeric APP to reduce the formation of substrate oligomers (Figure 10A–C) and to impair processing efficiency; and (iii) SORLA does not directly impact on enzymatic activity of secretases (Figures 8 and 9).

The reaction network was translated into a system of ordinary differential equations (ODEs), describing temporal changes of network components as a function of interactions and cleavage processes. The ODE model, its reduction and

the parameter values are presented in the Supplementary data. The parameter values of the model are estimated by optimization from dose-response series for sAPPα and sAPPβ as a function of APP_{tot} for cells with or without SORLA.

Simulations of the parameterized mathematical model are in good agreement with the experimental data (Figure 11B–E). The model combines monomer and dimer processing. The combined model has the lowest residual value (2.15×10^1 and

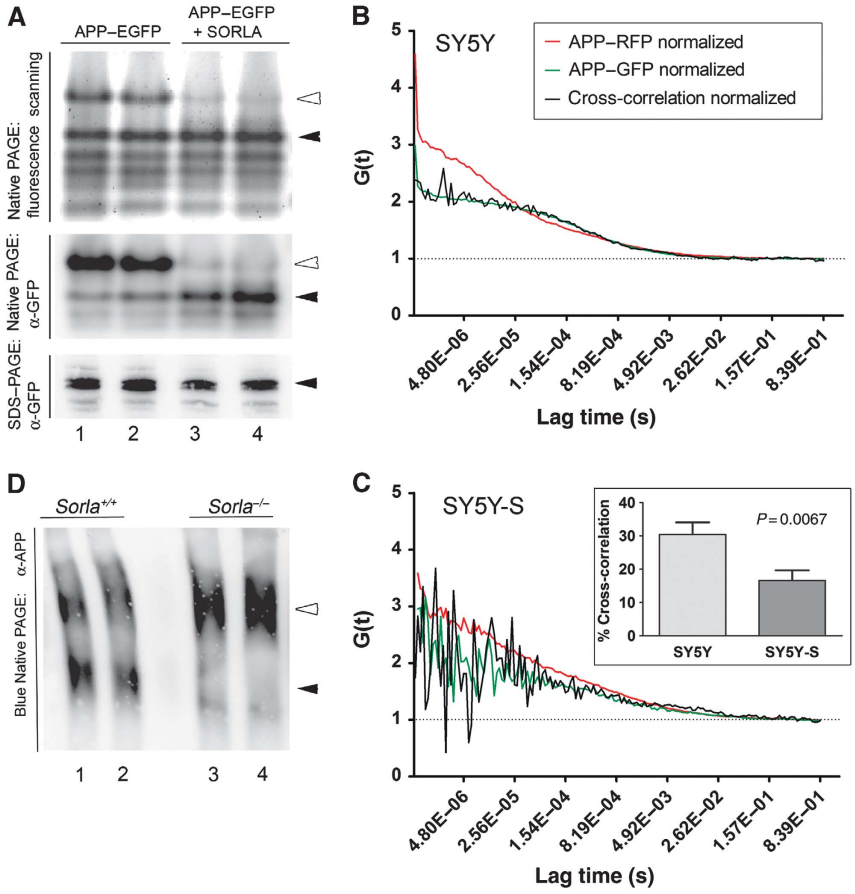

Figure 10 SORLA prevents oligomerization of APP in cultured cells and the brain *in vivo*. (**A**) Parental CHO cells (lanes 1 and 2) and CHO cells expressing 120 nM SORLA (CHO-S; lanes 3 and 4) were transiently transfected with expression constructs for APP–EGFP for 48 h. Subsequently, cell lysates were subjected to native PAGE and fluorescence scanning to detect EGFP activity (upper panel) or western blot analysis using anti-EGFP antisera (middle panel). As a control, replicate cell lysates were subjected to denaturing SDS–PAGE and western blotting with anti-GFP antisera (lower panel). Filled arrowheads indicate monomeric, open arrowheads present multimeric APP–EGFP forms. (**B**, **C**) SH-SY5Y cells were co-transfected with expression constructs for APP–GFP and APP–RFP. Two days later, cells were subjected to live cell imaging using FCS. Autocorrelation curves for APP–RFP (red lines) and APP–GFP (green lines) as well as for cross-correlation of fluorescence intensities in APP–GFP/APP–RFP heterodimers (black lines) are shown. The normalized cross-correlation curve in the absence of SORLA indicates substantial APP–GFP/APP–RFP heterodimer formation (**B**). In contrast, in SH-SY5Y cells expressing a SORLA transgene (SY5Y-S) (**C**), cross-correlation represents random noise, suggesting independent fluctuation of the two protein species. Using the ZEN Software 2010, the percent of dimer formation was shown to be reduced from 30 to 15% in the presence of SORLA (inset in **C**) (three independent repeats). (**D**) APP was immunoprecipitated from replicate brain samples from wild-type (lanes 1 and 2) or SORLA-deficient mice (lanes 3 and 4) and resolved by Blue Native PAGE. Immunoreactive bands corresponding to a low-molecular weight (filled arrowhead) and a high-molecular weight complex of APP (open arrowhead) are detected in wild-type tissues. Only the high-molecular weight complex of APP is seen in brain lacking SORLA (open arrowhead in lanes 3 and 4).

Figure 11 Mathematical modelling of APP processing and its influence by SORLA. (**A**) Biochemical network of the interaction of reactants APP (blue symbol) with α- and β-secretases (green symbols) and the formation of amyloidogenic and non-amyloidogenic products (orange symbols). Complexes of APP and secretases are indicated as white boxes and complexes of APP and SORLA as grey box. Processing of monomeric (upper panel) and of dimeric forms of APP (lower panel) is indicated as separate pathways. The two modules are linked together by the reversible dimerization-dissociation of APP and secretases. Interaction of SORLA with monomeric APP (grey box) has two consequences. It prevents formation of APP dimers, the preferred secretase substrates, and it lessens the amount of APP monomers available for processing. Note that dissociation of homodimers of APP (APP_d), α-secretase (α_d), and β-secretase (β_d) results in two identical monomers of the respective proteins. See Supplementary data for a detailed description of the variables used in the biochemical network. The diagram was produced with Cell Designer 4.0 (Cell Designer, Tokyo, Japan: The Systems Biology Institute; 2008) (Kitano *et al*, 2005). (**B**–**E**) Simulation results of the mathematical model (solid lines) for the various APP processing products are shown together with the actual data points obtained in biochemical experiments. The total amount of products (black line) is the sum of the products produced in the monomer (red line) and dimer processing (green line) pathways. In the absence of SORLA, the 'dimer processing' more closely resembles the combined model for sAPPα (**B**) and sAPPβ (**C**). In contrast, in the presence of SORLA, it is the 'monomer processing' that closely resembles the combined model for both processing products (**D**, **E**). In (**E**), black and red lines are superimposed.

3.10×10^1 for global-local and global parameter estimation, respectively; see Supplementary Table SA.4) as compared with a model with only monomer processing (best residual value 1.12×10^2) or a model with only dimer processing (best residual value 1.48×10^2). The comparison of models using statistical criteria, like the Akaike information criterion, requires standard deviations, which is why we used residuals to compare the models. In the absence of SORLA, the sigmoidal curve characteristic for dimer processing (green lines in Figure 11B and C) has a strong impact on the combined model (black lines in Figure 11B and C) that very well describes the experimental data sets for sAPPα

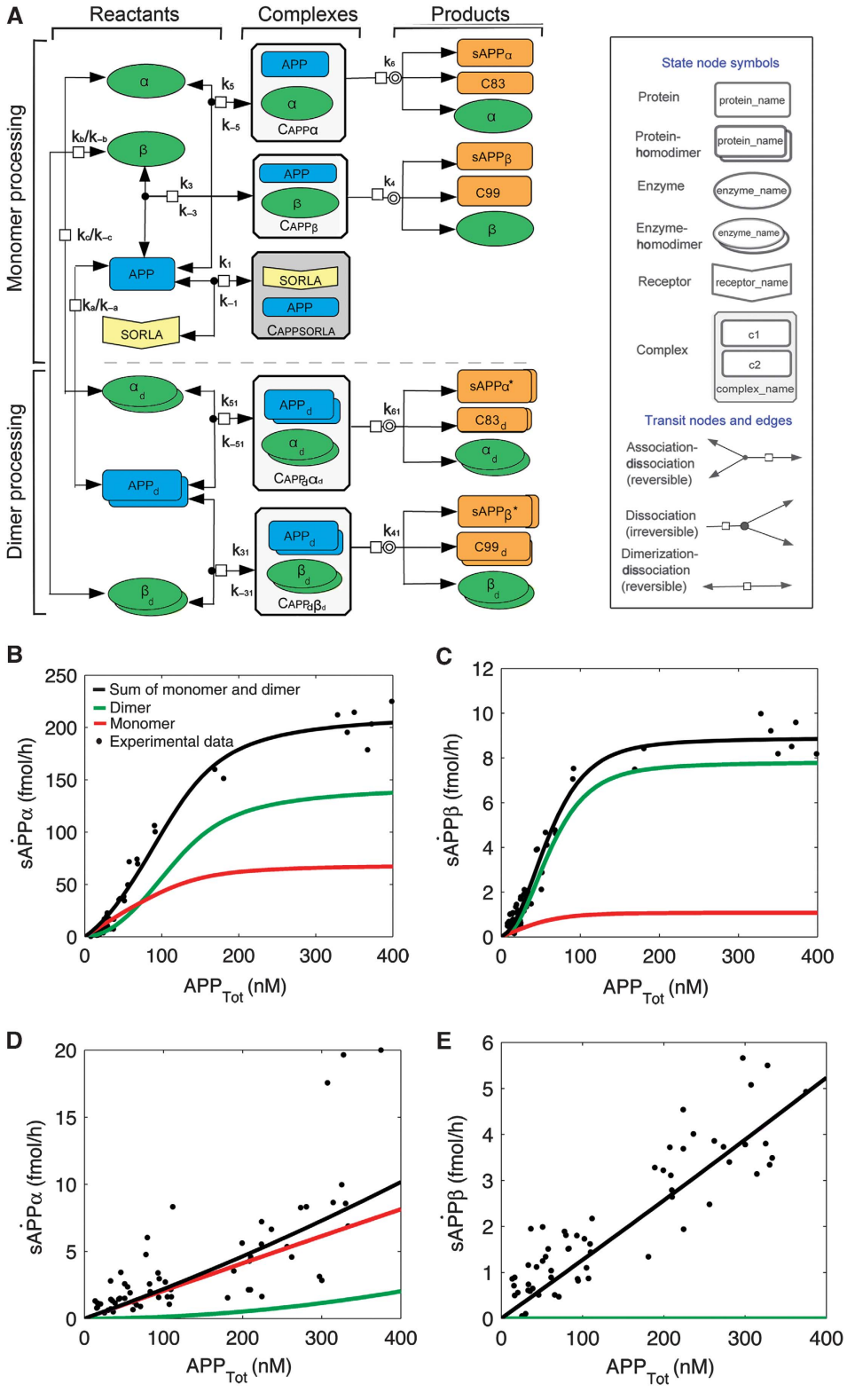

(black dots in Figure 11B) and sAPPβ (black dots in Figure 11C). In contrast, in the presence of the receptor, it is the monomer processing (red lines in Figure 11D and E) in the combined model (black lines in Figure 11D and E) that made the combined model closely resemble the experimental data for both sAPPα (black dots in Figure 11D) and sAPPβ (black dots in Figure 11E).

Up to this point, our model had considered the two most extreme scenarios with either no (Figure 11B and C) or high levels of SORLA activity (Figure 11D and E) as in CHO pTet-APP and CHO-S pTet-APP, respectively. However *in vivo*, subtle alterations in intermediary SORLA levels are likely more relevant for determination of APP processing rates. Accordingly, we next adapted our model to intermediary concentrations of SORLA to define when exactly the switch from cooperative to non-cooperative secretase activity may occur. To do so, we applied several approaches to estimate the relationship between SORLA concentration and quantitative parameter values for secretase activity as detailed in the Supplementary data. For these estimated parameter values, we simulated the dose-response kinetics of total sAPPα and sAPPβ production in dependence of three intermediate SORLA expression levels (3, 12, and 30% of $SORLA_{Tot}$ of CHO-S pTet-APP; Figure 12A and B). Based on these simulations, we predicted a switch from cooperative (dimer) to less efficient non-cooperative (monomer) processing to occur at a SORLA concentration that is $0.12\times$ $SORLA_{Tot}$ of CHO-S pTet-APP (where $SORLA_{Tot}$ equals 5.13×10^5 fmol) (Figure 12E and F).

Taken together, our quantitative biochemical data (Figure 3) and the simulations shown in Figures 11 and 12 strongly support a model whereby SORLA prevents oligomerization of APP, thereby shifting the mode of secretase action from use of the preferred homodimeric substrate to the less preferred monomer variant.

Discussion

Secretases are allosteric enzymes that require cooperativity from APP oligomers

Quantitative and qualitative changes in APP processing into Aβ peptides are considered causative of AD pathology (Haass and Selkoe, 2007). Using a combination of experimental data and mathematical modelling, we developed the first kinetic model describing proteolytic processing of APP through the concerted actions of α-, β-, and γ-secretases, and the influence of SORLA on these processes.

Remarkably, few experimental data exist describing the kinetics of APP processing in cells or *in vivo*. Most data are on cell-free assays with purified enzyme and artificial peptide substrate. Adopting Michaelis–Menten kinetics, rather poor kinetic constants for BACE1 were determined in these assays (K_m 4.5–7 μM) (Ermolieff *et al*, 2000; Gruninger-Leitch *et al*, 2002). Similarly, using Michaelis–Menten equation led to a $K_m = 0.47$ μM for γ-secretase in cell extracts (Tian *et al*, 2010).

Contrary to previous studies, we developed an assay to accurately describe the velocity of APP processing by all three secretases in the context of an intact cell. The first surprising finding came with the notion that α- and β-secretases do not follow Michaelis–Menten kinetics but constitute allosteric enzymes that require cooperativity for efficient processing (Figure 3). In the absence of SORLA, concentrations for APP at $\frac{1}{2}$ V_{max} (K') of 97.3 and 62.6 nM were determined for α- and β-secretases, respectively. Allosteric enzymes are characterized by the existence of several substrate-binding sites whereby occupation of the first site facilitates binding of the next substrate molecule by increasing the affinities of the vacant binding sites. As a consequence, the relationship between substrate concentration and enzyme velocity follows a sigmoidal rather than a hyperbolic relationship. Accordingly, allosteric enzymes act by an on–off switch mechanism enabling rapid adaptation of enzyme activity to even subtle changes in substrate concentration. This notion is exemplified for α-secretase herein, where an increase from 10% of V_{max} to 75% of V_{max} is achieved with only 4.4-fold increase in substrate concentration. Covering the same velocity range in the absence of cooperativity would require a 27-fold increase in APP concentration. Similarly for β-secretase in the absence of SORLA, the sigmoidal curve increases from 10% of V_{max} to 75% of V_{max} with only an additional 4.8-fold rise in substrate concentration. Use of APP (rather than CTFs) as the authentic substrate in our cell assay precludes direct assessment of γ-secretase activity. Still, $Aβ_{40}$ production in the absence of SORLA follows Hill characteristics, indicating that cooperativity also directly or indirectly determines the extent of Aβ production in the context of intact cells. This assumption is supported by a report demonstrating cooperativity (Hill coefficient = 2) for processing of C99-flag substrates in cell-free assays (Serneels *et al*, 2009). Our findings are intriguing in the light of previous observations implicating APP processing products in neuronal signalling pathways such as activation of NMDA receptors by sAPPα (Gakhar-Koppole *et al*, 2008) or induction of apoptosis (Yaar *et al*, 1997; Sotthibundhu *et al*, 2008) and control of synaptic transmission by Aβ (Kamenetz *et al*, 2003)—pathways that may depend on swift adaptive changes in signalling molecules.

SORLA blocks APP oligomerization and prevents cooperativity in processing

In terms of cooperativity, the Hill constant represents the combined effect of the actual number of ligand-binding sites and the strength of their interactions. Thus, $n = 2$ for α- and β-secretases (Table IA) may indicate two binding sites for APP with relative strong cooperativity but there could also be four sites with lesser cooperativity. Because homodimer formation has been documented for BACE1 (Benjannet *et al*, 2001; Schmechel *et al*, 2004; Westmeyer *et al*, 2004) and for APP (Scheuermann *et al*, 2001; Munter *et al*, 2007), we favour a model whereby pre-formed APP homodimers represent the favoured substrate for BACE1 (and possibly TACE or ADAM10) dimers (Figure 11A). This model is supported by the changes in K' ([APP] at $\frac{1}{2}$ V_{max}) from 97.3 to 5140.0 nM for α-secretase and 62.6 to 695.5 nM for β-secretase when comparing cells without (dimer processing) and with SORLA (monomer processing) (Figure 4).

As well as elucidating the kinetics and mode of secretase action, use of our cell model also enabled us to gain novel insights into the molecular mechanism of SORLA in APP processing. Thus, in the presence of SORLA, α- and β-secretases switch from an allosteric to a non-allosteric mode of action (Hill coefficient $\leqslant 1$), resulting in an 80–90% reduction in the production of soluble APPs and Aβ. Conceptually, SORLA may eliminate substrate cooperativity by physical interaction with the enzymes or the substrate.

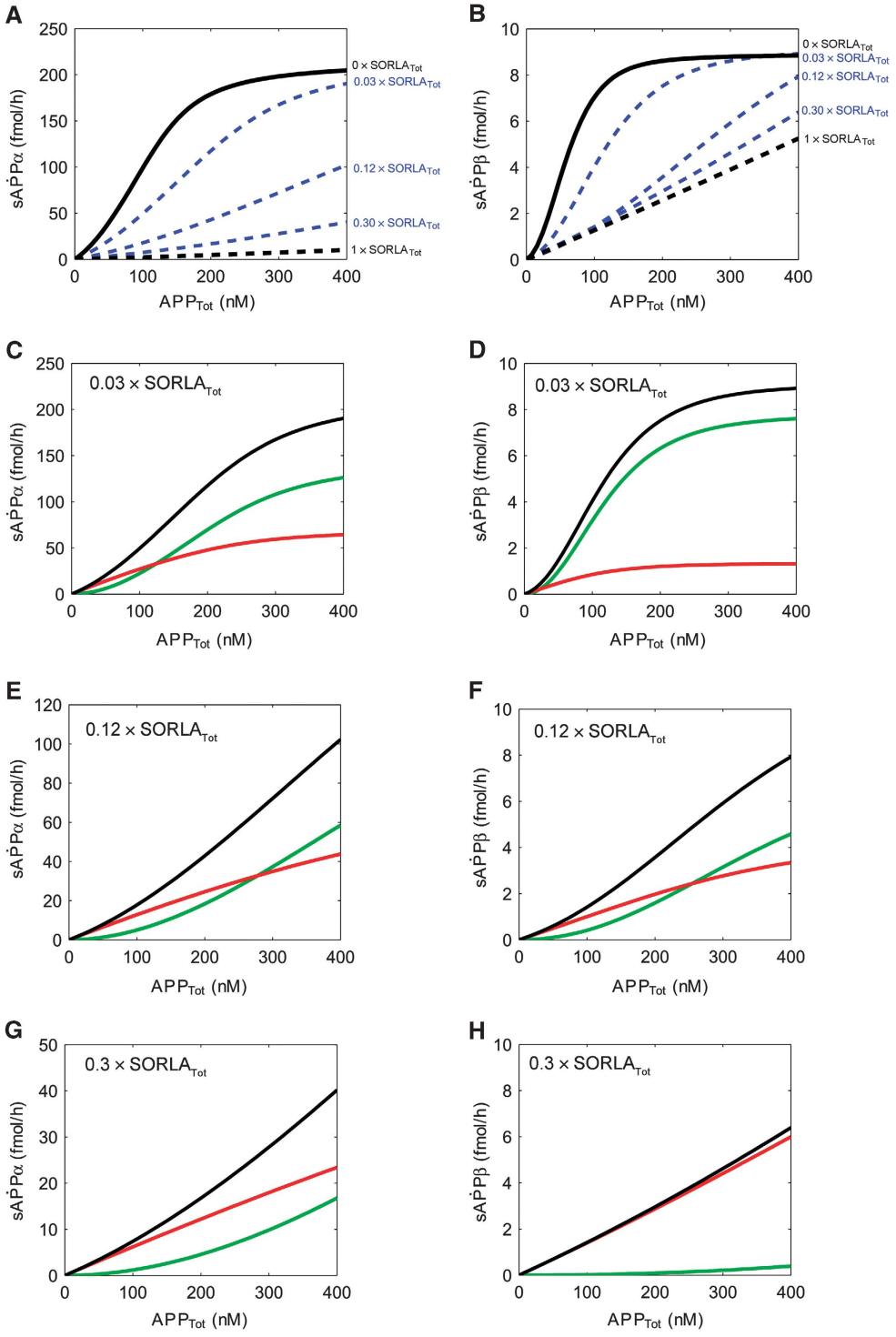

Figure 12 APP processing at intermediate levels of SORLA. (**A**, **B**) Simulations of the influence of intermediate levels of SORLA on APP processing into sAPPα (**A**) and sAPPβ (**B**) are shown. The stippled black lines in (**A**, **B**) represent the values for maximum levels of SORLA$_{Tot}$ (5.13×10^5 fmol) as in CHO-S pTet-APP (set at arbitrary value $1 \times$ SORLA$_{Tot}$). The solid black lines represent the situation in the absence of SORLA as in CHO pTet-APP (set at $0 \times$ SORLA$_{Tot}$). Simulations of total processing for three intermediates levels of SORLA (3, 12, and 30% of SORLA$_{Tot}$) were calculated as detailed in the Supplementary data, and are shown as blue stippled lines. (**C**–**H**) Simulation curves for APP processing into sAPPα and sAPPβ for intermediate levels of 3% (**C**, **D**), 12% (**E**, **F**), and 30% of SORLA$_{Tot}$ (**G**, **H**) are given. Total processing (black lines) as well as dimer (green lines) and monomer (red lines) processing are indicated for each simulation. A switch from preferred dimer-to-monomer processing is seen at $0.12 \times$ SORLA$_{Tot}$ for both α-secretase (**E**) and β-secretase (**F**).

However, the presence of high concentrations of SORLA in CHO-S pTet-APP did not directly impact the activity of α-, β-, or γ-secretases on artificial substrates in a cell-free assay (Figures 8 and 9), arguing that it is the interaction between receptor and substrate APP that is particularly relevant for inhibitory action.

Previous experimental evidence has highlighted the pathophysiological importance of APP dimerization. Approximately 30–50% of all APP molecules exist as homodimers (Munter *et al*, 2007). Dimerization occurs through two conserved homodimerization sites in the E1 and E2 domains of the extracellular portion of APP (Scheuermann *et al*, 2001; Wang and Ha, 2004; Kaden *et al*, 2008, 2009). That SORLA blocks formation of APP dimers is supported by findings that the interaction between both proteins proceeds via the cluster of complement type repeats in SORLA that bind to the carbohydrate-linked domain in the E2 region of APP (Andersen *et al*, 2006), the region essential for APP dimerization; and by the fact that APP and SORLA interact in a 1:1 stochiometric complex (Andersen *et al*, 2005). Finally, the ability of SORLA to sequester the monomeric form of APP thereby preventing dimer formation is confirmed by the lack of APP multimers in neuronal and non-neuronal cell lines expressing the inhibitor (Figure 10A–C) and by the accumulation of APP oligomers in the brains of mice genetically deficient for SORLA (Figure 10D).

With respect to the pathophysiological relevance, stabilization of APP dimers by introduction of an intermolecular disulphide bridge in the ectodomain results in a seven-fold increase in Aβ production (Scheuermann *et al*, 2001). More importantly, APP homodimers have been proposed to represent the substrate to produce dimeric C99 and, subsequently, dimeric Aβ species, neurotoxic variants of the Aβ peptide (Dyrks *et al*, 1992; El-Agnaf *et al*, 2000; Munter *et al*, 2007). Now, our data provide an explanatory model as they demonstrate that sequestration of APP dimers by SORLA deplete cells for the preferred secretase substrate resulting in >90% reduction in Aβ formation (Figure 5C). Whether or not the requirement for dimerization shown for APP here also applies to other physiological substrates of α- or β-secretases remains to be shown.

Minimal decline in SORLA activity contributes to amyloidogenic processing

Previous experimental evidence has demonstrated an inverse correlation of SORLA levels with APP processing rates. However, all of these data have been generated in cell lines overexpressing SORLA or in knockout models devoid of the receptor (Schmidt *et al*, 2007; Dodson *et al*, 2008; Rohe *et al*, 2008). Thus, it remained unclear whether a modest decrease of brain SORLA levels by 25% observed in patients may explain the occurrence of sporadic AD (Scherzer *et al*, 2004). Foremost, our studies confirmed a linear correlation between receptor levels and APP processing rates even at changes as small as those observed in humans. As shown both for CHO (Figure 6) and SH-SY5Y cells (Figure 7), changes in SORLA levels in our experimental models are *modest* and vary between two- and four-fold. Similar variations in the receptor levels are seen in patients with sporadic AD (two-fold) (Scherzer *et al*, 2004). Still, subtle changes in SORLA expression translate into highly significant alterations in APP processing rates over the entire concentration range as documented by linear regression analysis. According to the graphs for endogenous SORLA in SH-SY5Y cells, a two-fold reduction in receptor levels translates into a 30% increase in sAPPα and a 40% increase in sAPPβ production (Figure 7). Remarkably, similar increases in APP processing rates are observed in patients with sporadic AD (45% increase in sAPPα, 40% increase in sAPPβ) (Lewczuk *et al*, 2010). Likely, the allosteric mode of action of secretases ensures that even small changes in the availability of APP oligomers as determined by SORLA translate into major changes in processing rates.

Mathematical modelling confirms SORLA-dependent mode of secretase action

To this end, we have used the biochemical evidence gathered in this study to develop the first mathematical model describing the combined action of secretases and SORLA in APP processing. Obviously, this model represents a simplified view of APP processing as it considers a single cellular compartment. Clearly, regulated trafficking of APP by SORLA through the intracellular compartments critically affects amyloidogenic and non-amyloidogenic processing (reviewed in Willnow *et al*, 2008). Also, the observation that our model requires a local parameter estimate for β-secretase activity in the presence or absence of SORLA to closely resemble the experimental data (see Supplementary data for details) suggests that additional indirect effects of the receptor on this enzyme contribute to regulation of amyloidogenic processing in the context of an intact cell. Whether these effects entail interference of SORLA with the ability of BACE to bind APP (Spoelgen *et al*, 2006) or other yet unknown mechanisms remains to be elucidated.

Still, the fact that secretases switch their mode of action in the presence of the receptor demonstrates that its function is more complex than simply preventing transport of APP into compartments where the enzymes reside. Good agreement of the mathematical model with the experimental data strongly argues that depletion of APP dimer processing represents a major molecular mechanism whereby SORLA affects APP processing fates. Conceptually, this model represents a unique tool to map the quantitative contribution of additional *cis*-acting factors to APP processing and perhaps even to stratify the amyloidogenic burden in individuals with a given ratio of APP and SORLA.

Materials and methods

Materials

Antisera for detection of SORLA and of a carboxyl terminal peptide in APP and its processing products (IgG 1227) have been described before (Schmidt *et al*, 2007). Antibodies directed against mouse APP (6E10; Covance), actin (Sigma), tubulin (Calbiochem), BACE1 (Biomol GmbH), TACE, and ADAM10 (Chemicon International), as well as GFP (Abcam) were obtained from commercial suppliers.

Cell culture

CHO cells constitutively overexpressing human SORLA (CHO-S) or human APP_{695} (CHO-A) have been published (Schmidt *et al*, 2007). For doxycyline-regulatable expression, the respective cDNAs were cloned into vector pTRE2pur and co-transfected with pTet-Off vector pUHD15-1neo into CHO cells (Gossen and Bujard, 1992). To control gene expression, 0.025–10 ng/ml doxycycline (Clonetech Laboratories) was added to the culture medium for 24 h for CHO-pTet-APP cells or for 48 h for CHO-pTet-SORLA. Quantification of proteins by western blot and ELISA is described in the Supplementary data. Enzyme kinetics were determined using lsq nonlin in Matlab 7.6.0. Knockdown of SORLA expression by siRNA as well as FCS analysis in the neuroblastoma cell lines SH-SY5Y is described in the Supplementary data.

Secretase assays

Commercially available assays were used to determine the activities of α-secretase (SensoLyte 520 TACE Activity Assay Kit; AnaSpec)

and β-secretase (BioVision). To quantify γ-secretase activity, constructs encoding C99 and C83 were transiently introduced into CHO and CHO-S cells for 48 h. Thereafter, cells were lysed and divided into two equal parts. Whereas one aliquot was kept on ice (0 time point), the second aliquot was incubated at 37 °C for 2 h. Thereafter, lysates were subjected to immunodetection of C99, C83, and AICD using anti-APP IgG 1227 as described in the Supplementary data.

Native SDS–PAGE

For detection of APP dimers in cells, CHO and CHO-S cells were transiently transfected with construct pcDNA3.1hyg APP695–eGFP. After 48 h, protein lysates were generated using lysis buffer without detergents (50 mM Tris, pH 8.0) and subjected to 6% native Tris-Glycine polyacrylamide gels without SDS. Electrophoresis was performed in running buffer (125 mM Tris, 960 mM Glycine) at 20–25 mA at 4 °C. Separated APP–eGFP proteins in the gels were scanned by FLA-3000 Fujifilm with BAS Reader 3.14 software at 488 nm before subjecting them to transfer onto nitrocellulose membranes in 1% SDS-containing buffer and standard western blot analysis.

For detection of APP dimers *in vivo*, mouse brain tissue was homogenized in lysis buffer (250 mM sucrose, 5 mM HEPES/NaOH, pH 7.4, 1 mM $MgCl_2$, 10 mM KCl). The cell membrane fraction was collected by centrifugation (800 *g*, 10 min, 4 °C) and resuspended in cross-linking buffer (150 mM NaCl, 20 mM HEPES/NaOH, pH 7.5) containing 1 mM dithiobis (sulfosuccinimidyl) propionate (DTSSP) (Pierce). After incubation for 1 h at room temperature, cross-linking was stopped by adjusting the solution to 50 mM Tris–HCl (pH 7.5) and further incubation for 30 min. Thereafter, detergents Nonidet P-40 and Triton X-100 were added to a final concentration of 2% each, and APP was immunoprecipitated using IgG 1227 and protein G-agarose beads (Roche Molecular Biochemicals). Immunoprecipitated proteins were analysed by Blue Native PAGE (Novex 3–12% Bis-Tris Gels; Invitrogen) according to the manufacturer's protocols.

Mathematical modelling of APP processing

A detailed description of mathematical modelling of APP processing is given in the Supplementary data.

Supplementary data

Supplementary data are available at *The EMBO Journal* Online (http://www.embojournal.org).

Acknowledgements

We are indebted to Gerd Multhaup (Free University of Berlin) for critical discussions, to Manfred Gossen (MDC, Berlin) for providing pTet constructs, to Anja Bauerfeind (MDC, Berlin) for help with the statistical analysis, and to Christine Kruse for expert technical assistance. Studies in this project were funded in part by a MSBN grant from the Helmholtz-Association (to TW, OW, JW, and KR) and by the BMBF FORSYS partner program (Grant number 0315255; to KR).

Author contributions: VS conducted all cell and molecular biology experiments. VS and KB performed the analyses of enzyme kinetics. AL, KR, and YS carried out the mathematical modelling. AT and BW performed the live cell imaging studies. CMP provided essential reagents for the SORLA ELISA. AN, JW, OW, and TEW conceived the experiments. TEW wrote the manuscript.

Conflict of interest

The authors declare that they have no conflict of interest.

References

Andersen OM, Reiche J, Schmidt V, Gotthardt M, Spoelgen R, Behlke J, von Arnim CA, Breiderhoff T, Jansen P, Wu X, Bales KR, Cappai R, Masters CL, Gliemann J, Mufson EJ, Hyman BT, Paul SM, Nykjaer A, Willnow TE (2005) Neuronal sorting protein-related receptor sorLA/LR11 regulates processing of the amyloid precursor protein. *Proc Natl Acad Sci USA* **102:** 13461–13466

Andersen OM, Schmidt V, Spoelgen R, Gliemann J, Behlke J, Galatis D, McKinstry WJ, Parker MW, Masters CL, Hyman BT, Cappai R, Willnow TE (2006) Molecular dissection of the interaction between amyloid precursor protein and its neuronal trafficking receptor SorLA/LR11. *Biochemistry* **45:** 2618–2628

Benjannet S, Elagoz A, Wickham L, Mamarbachi M, Munzer JS, Basak A, Lazure C, Cromlish JA, Sisodia S, Checler F, Chretien M, Seidah NG (2001) Post-translational processing of beta-secretase (beta-amyloid-converting enzyme) and its ectodomain shedding. The pro- and transmembrane/cytosolic domains affect its cellular activity and amyloid-beta production. *J Biol Chem* **276:** 10879–10887

Dodson SE, Andersen OM, Karmali V, Fritz JJ, Cheng D, Peng J, Levey AI, Willnow TE, Lah JJ (2008) Loss of LR11/SORLA enhances early pathology in a mouse model of amyloidosis: evidence for a proximal role in Alzheimer's disease. *J Neurosci* **28:** 12877–12886

Dodson SE, Gearing M, Lippa CF, Montine TJ, Levey AI, Lah JJ (2006) LR11/SorLA expression is reduced in sporadic Alzheimer disease but not in familial Alzheimer disease. *J Neuropathol Exp Neurol* **65:** 866–872

Dyrks T, Dyrks E, Masters C, Beyreuther K (1992) Membrane inserted APP fragments containing the beta A4 sequence of Alzheimer's disease do not aggregate. *FEBS Lett* **309:** 20–24

El-Agnaf OM, Mahil DS, Patel BP, Austen BM (2000) Oligomerization and toxicity of beta-amyloid-42 implicated in Alzheimer's disease. *Biochem Biophys Res Commun* **273:** 1003–1007

Elson EL (2001) Fluorescence correlation spectroscopy measures molecular transport in cells. *Traffic* **2:** 789–796

Ermolieff J, Loy JA, Koelsch G, Tang J (2000) Proteolytic activation of recombinant pro-memapsin 2 (pro-beta-secretase) studied with new fluorogenic substrates. *Biochemistry* **39:** 12450–12456

Gakhar-Koppole N, Hundeshagen P, Mandl C, Weyer SW, Allinquant B, Muller U, Ciccolini F (2008) Activity requires soluble amyloid precursor protein alpha to promote neurite outgrowth in neural stem cell-derived neurons via activation of the MAPK pathway. *Eur J Neurosci* **28:** 871–882

Gossen M, Bujard H (1992) Tight control of gene expression in mammalian cells by tetracycline-responsive promoters. *Proc Natl Acad Sci USA* **89:** 5547–5551

Gruninger-Leitch F, Schlatter D, Kung E, Nelbock P, Dobeli H (2002) Substrate and inhibitor profile of BACE (beta-secretase) and comparison with other mammalian aspartic proteases. *J Biol Chem* **277:** 4687–4693

Haass C, Selkoe DJ (2007) Soluble protein oligomers in neurodegeneration: lessons from the Alzheimer's amyloid beta-peptide. *Nat Rev Mol Cell Biol* **8:** 101–112

Hardy J (2009) The amyloid hypothesis for Alzheimer's disease: a critical reappraisal. *J Neurochem* **110:** 1129–1134

Kaden D, Munter LM, Joshi M, Treiber C, Weise C, Bethge T, Voigt P, Schaefer M, Beyermann M, Reif B, Multhaup G (2008) Homophilic interactions of the amyloid precursor protein (APP) ectodomain are regulated by the loop region and affect beta-secretase cleavage of APP. *J Biol Chem* **283:** 7271–7279

Kaden D, Voigt P, Munter LM, Bobowski KD, Schaefer M, Multhaup G (2009) Subcellular localization and dimerization of APLP1 are strikingly different from APP and APLP2. *J Cell Sci* **122:** 368–377

Kamenetz F, Tomita T, Hsieh H, Seabrook G, Borchelt D, Iwatsubo T, Sisodia S, Malinow R (2003) APP processing and synaptic function. *Neuron* **37:** 925–937

Kitano H, Funahashi A, Matsuoka Y, Oda K (2005) Using process diagrams for the graphical representation of biological networks. *Nat Biotechnol* **23:** 961–966

Lewczuk P, Kamrowski-Kruck H, Peters O, Heuser I, Jessen F, Popp J, Burger K, Hampel H, Frolich L, Wolf S, Prinz B, Jahn H, Luckhaus C, Perneczky R, Hull M, Schroder J, Kessler H, Pantel J, Gertz HJ, Klafki HW *et al* (2010) Soluble amyloid precursor proteins in the cerebrospinal fluid as novel potential biomarkers of Alzheimer's disease: a multicenter study. *Mol Psychiatry* **15:** 138–145

Matsuda S, Giliberto L, Matsuda Y, Davies P, McGowan E, Pickford F, Ghiso J, Frangione B, D'Adamio L (2005) The familial dementia BRI2 gene binds the Alzheimer gene amyloid-beta precursor protein and inhibits amyloid-beta production. *J Biol Chem* **280:** 28912–28916

Munter LM, Voigt P, Harmeier A, Kaden D, Gottschalk KE, Weise C, Pipkorn R, Schaefer M, Langosch D, Multhaup G (2007) GxxxG motifs within the amyloid precursor protein transmembrane sequence are critical for the etiology of Abeta42. *EMBO J* **26:** 1702–1712

Offe K, Dodson SE, Shoemaker JT, Fritz JJ, Gearing M, Levey AI, Lah JJ (2006) The lipoprotein receptor LR11 regulates amyloid beta production and amyloid precursor protein traffic in endosomal compartments. *J Neurosci* **26:** 1596–1603

Park JH, Strittmatter SM (2007) Nogo receptor interacts with brain APP and Abeta to reduce pathologic changes in Alzheimer's transgenic mice. *Curr Alzheimer Res* **4:** 568–570

Pietrzik CU, Busse T, Merriam DE, Weggen S, Koo EH (2002) The cytoplasmic domain of the LDL receptor-related protein regulates multiple steps in APP processing. *EMBO J* **21:** 5691–5700

Rogaeva E, Meng Y, Lee JH, Gu Y, Kawarai T, Zou F, Katayama T, Baldwin CT, Cheng R, Hasegawa H, Chen F, Shibata N, Lunetta KL, Pardossi-Piquard R, Bohm C, Wakutani Y, Cupples LA, Cuenco KT, Green RC, Pinessi L *et al* (2007) The neuronal sortilin-related receptor SORL1 is genetically associated with Alzheimer disease. *Nat Genet* **39:** 168–177

Rohe M, Carlo AS, Breyhan H, Sporbert A, Militz D, Schmidt V, Wozny C, Harmeier A, Erdmann B, Bales KR, Wolf S, Kempermann G, Paul SM, Schmitz D, Bayer TA, Willnow TE, Andersen OM (2008) Sortilin-related receptor with A-type repeats (SORLA) affects the amyloid precursor protein-dependent stimulation of ERK signaling and adult neurogenesis. *J Biol Chem* **283:** 14826–14834

Scherzer CR, Offe K, Gearing M, Rees HD, Fang G, Heilman CJ, Schaller C, Bujo H, Levey AI, Lah JJ (2004) Loss of apolipoprotein E receptor LR11 in Alzheimer disease. *Arch Neurol* **61:** 1200–1205

Scheuermann S, Hambsch B, Hesse L, Stumm J, Schmidt C, Beher D, Bayer TA, Beyreuther K, Multhaup G (2001) Homodimerization of amyloid precursor protein and its implication in the amyloidogenic pathway of Alzheimer's disease. *J Biol Chem* **276:** 33923–33929

Schmechel A, Strauss M, Schlicksupp A, Pipkorn R, Haass C, Bayer TA, Multhaup G (2004) Human BACE forms dimers and colocalizes with APP. *J Biol Chem* **279:** 39710–39717

Schmidt V, Sporbert A, Rohe M, Reimer T, Rehm A, Andersen OM, Willnow TE (2007) SorLA/LR11 regulates processing of amyloid precursor protein via interaction with adaptors GGA and PACS-1. *J Biol Chem* **282:** 32956–32964

Serneels L, Van Biervliet J, Craessaerts K, Dejaegere T, Horre K, Van Houtvin T, Esselmann H, Paul S, Schafer MK, Berezovska O, Hyman BT, Sprangers B, Sciot R, Moons L, Jucker M, Yang Z, May PC, Karran E, Wiltfang J, D'Hooge R *et al* (2009) gamma-Secretase heterogeneity in the Aph1 subunit: relevance for Alzheimer's disease. *Science* **324:** 639–642

Sotthibundhu A, Sykes AM, Fox B, Underwood CK, Thangnipon W, Coulson EJ (2008) Beta-amyloid(1-42) induces neuronal death through the p75 neurotrophin receptor. *J Neurosci* **28:** 3941–3946

Spoelgen R, von Arnim CA, Thomas AV, Peltan ID, Koker M, Deng A, Irizarry MC, Andersen OM, Willnow TE, Hyman BT (2006) Interaction of the cytosolic domains of sorLA/LR11 with the amyloid precursor protein (APP) and beta-secretase beta-site APP-cleaving enzyme. *J Neurosci* **26:** 418–428

Tian Y, Bassit B, Chau D, Li YM (2010) An APP inhibitory domain containing the Flemish mutation residue modulates gamma-secretase activity for Abeta production. *Nat Struct Mol Biol* **17:** 151–158

Wang Y, Ha Y (2004) The X-ray structure of an antiparallel dimer of the human amyloid precursor protein E2 domain. *Mol Cell* **15:** 343–353

Westmeyer GG, Willem M, Lichtenthaler SF, Lurman G, Multhaup G, Assfalg-Machleidt I, Reiss K, Saftig P, Haass C (2004) Dimerization of beta-site beta-amyloid precursor protein-cleaving enzyme. *J Biol Chem* **279:** 53205–53212

Willnow TE, Petersen CM, Nykjaer A (2008) VPS10P-domain receptors—regulators of neuronal viability and function. *Nat Rev Neurosci* **9:** 899–909

Yaar M, Zhai S, Pilch PF, Doyle SM, Eisenhauer PB, Fine RE, Gilchrest BA (1997) Binding of beta-amyloid to the p75 neurotrophin receptor induces apoptosis. A possible mechanism for Alzheimer's disease. *J Clin Invest* **100:** 2333–2340

